Clinical Ophthalmology

Dovepress
open access to scientific and medical research

Open Access Full Text Article

ORIGINAL RESEARCH

Simulation of Changes in Tensile Strain by Airbag Impact on Eyes After Trabeculectomy by Using Finite Element Analysis

Shuji Suzuki[1], Aya Ikeda[1], Takashi Uemura[1], Kazuhiro Harada[1], Rie Takahashi[1], Jane Huang[1], Tomoko Tsukahara-Kawamura[1], Hiroaki Ozaki[1], Kazuaki Kadonosono[2], Eiichi Uchio[1]

[1]Department of Ophthalmology, Fukuoka University School of Medicine, Fukuoka, Japan; [2]Department of Ophthalmology, Yokohama City University Medical Center, Yokohama, Japan

Correspondence: Eiichi Uchio, Department of Ophthalmology, Fukuoka University School of Medicine, 7-45-1 Nanakuma, Jonan, Fukuoka, 814-0180, Japan, Email euchio@fukuoka-u.ac.jp

Purpose: We studied the kinetic phenomenon of an airbag impact on eyes after trabeculectomy using finite element analysis (FEA), a computerized method for predicting how an object reacts to real-world physical effects and showing whether an object will break, to sequentially determine the responses at various airbag deployment velocities.

Methods: A human eye model was used in the simulations using the FEA program PAM-GENERIS™ (Nihon ESI, Tokyo, Japan). A half-thickness incised scleral flap was created on the limbus and the strength of its adhesion to the outer sclera was set at 30%, 50%, and 100%. The airbag was set to hit the surface of the post-trabeculectomy eye at various velocities in two directions: perpendicular to the corneal center or perpendicular to the scleral flap (30° gaze-down position), at initial velocities of 20, 30, 40, 50, and 60 m/s.

Results: When the airbag impacted at 20 m/s or 30 m/s, the strain on the cornea and sclera did not reach the mechanical threshold and globe rupture was not observed. Scleral flap lacerations were observed at 40 m/s or more in any eye position, and scleral rupture extending posteriorly from the scleral flap edge and rupture of the scleral flap resulting from extension of the corneal laceration through limbal damage were observed. Even in the case of 100% scleral flap adhesion strength, scleral flap rupture occurred at 50 m/s impact velocity in the 30° gaze-down position, whereas in eyes with 30% or 50% scleral flap adhesion strength, scleral rupture was observed at an impact velocity of 40 m/s or more in both eye positions.

Conclusion: An airbag impact of ≥40 m/s might induce scleral flap rupture, indicating that current airbags may induce globe rupture in the eyes after trabeculectomy. The considerable damage caused by an airbag on the eyes of short-stature patients with glaucoma who have undergone trabeculectomy might indicate the necessity of ocular protection to avoid permanent eye damage.

Keywords: airbag, trabeculectomy, sclera, flap, rupture, finite element analysis

Introduction

Airbags protect passengers from road traffic collisions by absorbing the sudden impact caused, and they have substantially reduced mortality and morbidity since their introduction in the 1980s.[1] However, the survivors saved by airbags may suffer various fatal and nonfatal injuries of the head, eyes, neck, chest, or arms due to the high airbag deployment velocities of up to 200 mph.[2,3] An airbag impact may result in severe ocular damage with significant loss of vision.[4] Ocular injuries caused by airbags have been widely reported in the literature, such as corneal abrasion, corneoscleral laceration, hyphema, lens dislocation, lens capsule rupture, choroidal rupture, retinal tear, retinal detachment, and open globe rupture.[5–13]

Glaucoma is a chronic neurodegenerative optic nerve disease. Treatment is aimed at preventing the development and progression of optic nerve damage by lowering the intraocular pressure (IOP). Current therapeutic options include topical/systemic drugs, laser therapy and incisional surgery. The importance of and need for incisional surgery have decreased due to the refinement of medical and laser treatment. More recently, less invasive glaucoma procedures, collectively termed MIGS (minimally invasive glaucoma surgery), have gained popularity, with new devices regularly entering the market.[14]

Received: 16 January 2024
Accepted: 24 April 2024
Published: 14 May 2024

Trabeculectomy as well as the use of glaucoma drainage devices, has been frequently performed for several decades in Japan, given their high efficacy in lowering IOP especially in cases refractory to other treatments. Therefore, there remain a considerable number of patients who have undergone trabeculectomy. During trabeculectomy, a "fistula" is created between the anterior chamber and the sub-tenon space to allow aqueous humor to bypass the trabecular meshwork. An opening (ostomy) is made in the corneoscleral tissue situated at the level of the trabecular meshwork. This ostomy is covered by a scleral flap; however, the tightness of the flap sutures results in variable resistance and hence lack of standardization. Incisional surgery such as trabeculectomy reduces the resistance of the eye to trauma.[15] The use of antimetabolites such as 5-fluorouracil and mitomycin C during trabeculectomy has become almost routine, and antimetabolites have markedly improved the success rate in patients at high risk of trabeculectomy failure, thereby reducing the need for postoperative glaucoma medication.[16] However, they increase the risk of complications, such as bleb leaks, maculopathy, hypotony,[17] and scleral melting in the late phase[15] due to the inhibition of fibroblast proliferation and collagen fiber regrowth,[18] leading to the sclera being more susceptible to strain by blunt trauma, as observed in a case of traumatic scleral flap rupture 6 years after trabeculectomy.[19] Ingrowth of fibroblasts and cross-linking of collagen fibers induce adhesion between the scleral flap and the surrounding sclera; however, it was observed that the scleral flap did not adhere to the scleral wound bed on histological observation.[18] Several cases of blunt trauma injuries of the eye after trabeculectomy, such as scleral flap dehiscence with Valsalva maneuver,[15] late traumatic scleral flap dehiscence[20] or scleral rupture by an opening car door,[21] have also been reported. However, as far as we surveyed, no study has evaluated the mechanical behavior of tissues in eyes that have undergone trabeculectomy, including a scleral flap, following blunt trauma.

Creating a human-like eye with raw data from the human eye for biomechanical simulations using finite element analysis (FEA) would help to investigate and better explain the physical and physiological ocular responses to impact injuries.[22] We have previously developed a simulation model resembling a human eye[23] and applied three-dimensional FEA to determine the physical and mechanical response of the eyeball to an impacting airbag or airsoft gun projectile.[24–30] The important benefits of computer models to analyze biomechanical experiments and to quantify mechanical parameters are that we can evaluate the tensile strain of ocular segments by freely changing the impacting velocity or ocular tissue properties and they may reduce the need for animal studies, which are being increasingly restricted on ethical grounds.

Although blunt trauma to the eye after trabeculectomy has been reported in several studies,[19,31] it is difficult to simulate the situations of these reported cases, such as being beaten with a fist,[19] or hitting against the edge of a table,[31] while corneoscleral laceration due to airbag deployment has been reported,[6,32] but no case of serious blunt trauma of eyes after trabeculectomy has been reported. Therefore, we selected the eye after trabeculectomy in this FEA airbag eye-impact study as a simulation model for the kinetic phenomena in the eye with an incision at the corneoscleral border. In this study, we performed FEA of changes in tensile strain caused by airbag impact on the eyes after trabeculectomy at various deployment velocities to survey the mechanical threshold in these eyes. Reproducing the kinetic phenomena and deformation caused by airbag impact on eyes that had undergone trabeculectomy would increase our understanding of the risk of corneoscleral damage and possible globe rupture in these cases.

Materials and Methods

We employed a model of the human eye as reported previously,[23] in computer simulations using the FEA program PAM-GENERIS™ (Nihon ESI, Tokyo, Japan).[23] Poisson ratio of the cornea of 0.420 and of the sclera of 0.470, which were simulated as elastic components, were used to determine the standard tensile strain curves for the cornea and sclera.[33,34] For simplification, the cornea was spherical with a central thickness of 0.5 mm and radius of curvature of 7.80 mm. Thickness of the sclera was varied between 0.3 mm (equatorial segment) and 1.0 mm (posterior pole) according to the location. The anterior chamber was set at a depth of 5.1 mm, the vitreous length was assumed to be 18.6 mm, and the posterior curvature of the retina was assumed to be 12.0 mm in this model.[23] A vitreous model as a solid mass with a hydrostatic pressure of 20 mmHg (2.7 kPa) was also assigned.[29] Mass density and mesh principles of each tissue were similar to those in our recent study.[30] Axial length was set at 23.85 mm.

A half-thickness incised scleral flap is created in the limbus. The size of a scleral flap varies clinically; however, a trapezoid with lower base of 3.6 mm, upper base of 5.0 mm, and two lateral sides of 3.0 mm was used in this simulation, because of the scleral mesh size. To simulate the varying strengths of the scleral flap, the adhesion strength of the scleral flap to the surrounding sclera was set at 30%, 50%, and 100%, indicating the strength of the flap during the postsurgical stage. The location of the incised scleral flap area is highlighted in bold in the slow-motion image results.

The first step involved modifying the Hybrid III model[35] by replacing the head of the dummy with a biomechanical model of the head in which the eyeball model was inserted, as shown in Figure 1, where everything excluding the eye was a solid element, to reduce the computing time. The impact velocity of airbags has been reported to range from 100 mph to 200 mph, with an average velocity of 144 mps (64.5 m/s).[36] Airbag deployment velocities have been calculated physically in the range from 100 km/h to 300 km/h (approximately 28 m/s to 83 m/s).[37] Based on these reports on the velocity of airbag deployment,[36,37] impact velocities of the airbag patch on the face were 20, 30, 40, 50, and 60 m/s in this study. The airbag was set to hit the surface of the post-trabeculectomy eye in two directions: perpendicular to the corneal center (straight position) or perpendicular to the scleral flap (30° gaze-down position). The most likely position for the eye will be in upward-gaze during eye closure; however, a downward-gaze down position was selected to survey the effect of a direct airbag impacting force in this study.

It is assumed that globe rupture occurs at a strain of 18.0% in the cornea and 6.8% in the sclera at a stress of 9.4 MPa for both tissues. If the strain exceeded the tensile tolerance threshold, the tissues were displayed as lucent tissue in a light gray color in the element deletion method.[23] Changes in the shape of the eye and the induced strain were calculated using a virtual performance solver (VPS) (Nihon ESI) and evaluated by color mapping (Figure 2). The strain and size relationships are displayed graphically in slow motion. The mean strain of 50 simulation situations was considered as the strain on the cornea and sclera.

Results

The adhesion strength of the scleral flap was set at three strengths, 30%, 50%, and 100%, and the airbag impact velocity was set at five velocities, 20, 30, 40, 50, and 60 m/s. The airbag was set to hit the surface of the post-trabeculectomy eye in two directions: straight position and 30° gaze-down position. Therefore, 30 cases were simulated in this study. In each case, tensile strain changes were displayed at 0.2-ms intervals until the end of the simulation (2.0 ms after the impact). The threshold of tensile strain for the cornea and sclera was 18.0% and 6.8%, respectively; therefore, if the color turned red (0.16) in the cornea, it indicated corneal rupture, and if the color changed to green (0.067), it indicated scleral rupture including the scleral flap region.

When the airbag was impacted at 20 m/s or 30 m/s, the strains of the cornea and sclera did not reach the threshold, and globe rupture was not observed in this simulation. Therefore, the results of the cases in the 30° gaze-down position at an impact velocity of 40 m/s or more are shown in Figures 3–11, and those in the straight position are shown in Figures 12–20. From the outlined observation of these results, firstly, corneal (Figures 2–18) or scleral (Figures 2, 3, 5, 6, 8 and 9) lacerations occurred at higher

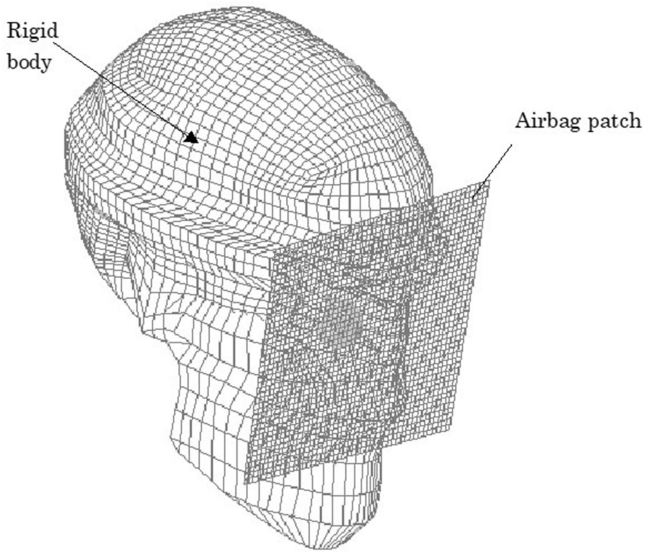

Figure 1 Biomechanical model of head. Parts other than the eye were assumed to be rigid elements, and the impacting object was placed adjacent to the eyeball to reduce the computing time of the airbag impact simulation.

Figure 2 Deformation scale in simulation Color mapping scale of deformation of eye showing strain induced; warmer color of red represents greater deformation.

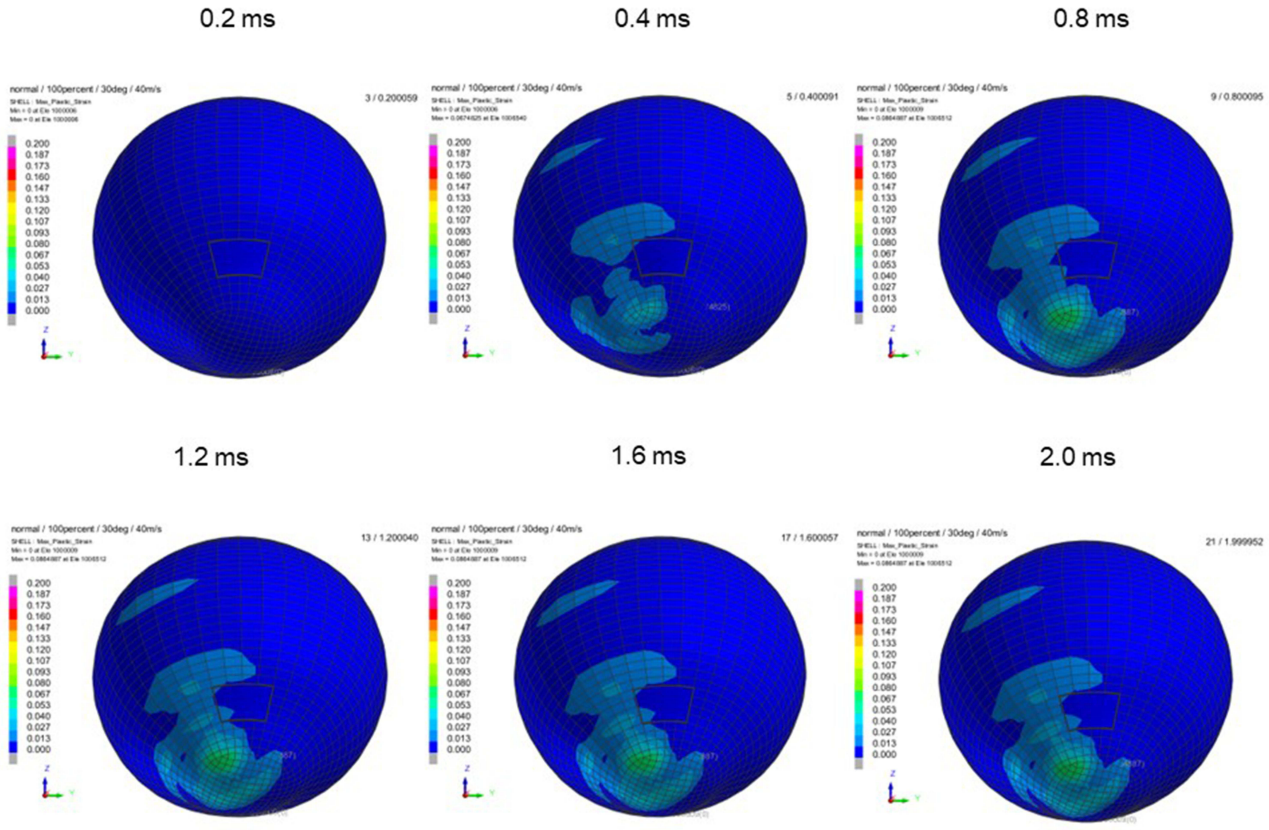

Figure 3 Sequential strain strength response of ocular surface of model eye upon airbag impact in 30° gaze-down position at 40 m/s with adhesion strength of scleral flap of 100%, shown in 0.4-ms intervals after 0.2 ms. Strain strength change is displayed in color as presented in the color bar scale (Figure 2).

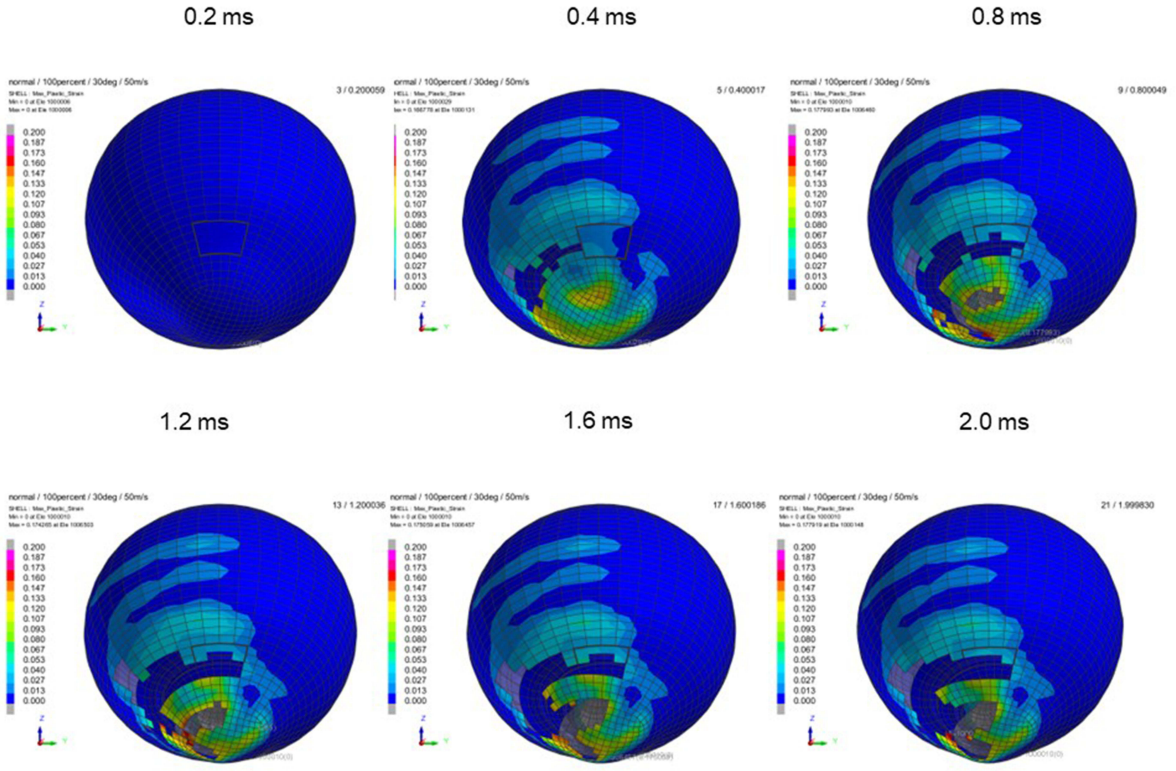

Figure 4 Sequential strain strength response of ocular surface of model eye upon airbag impact in 30°-gaze down position at 50 m/s with adhesion strength of scleral flap of 100%, shown at 0.4-ms intervals after 0.2 ms. Strain strength change is displayed in color as presented in the color bar scale (Figure 2).

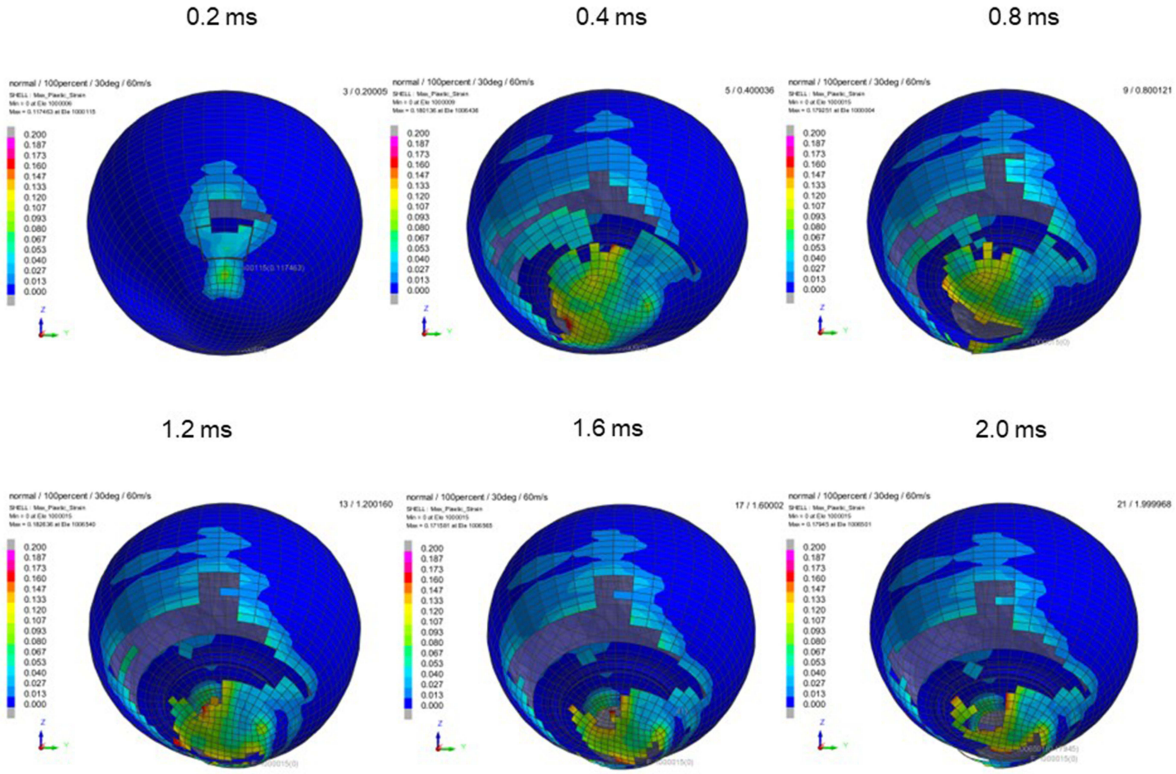

Figure 5 Sequential strain strength response of ocular surface of model eye upon airbag impact in 30°-gaze down position at 60 m/s with adhesion strength of scleral flap of 100%, shown at 0.4-ms intervals after 0.2 ms. Strain strength change is displayed in color as presented in the color bar scale (Figure 2).

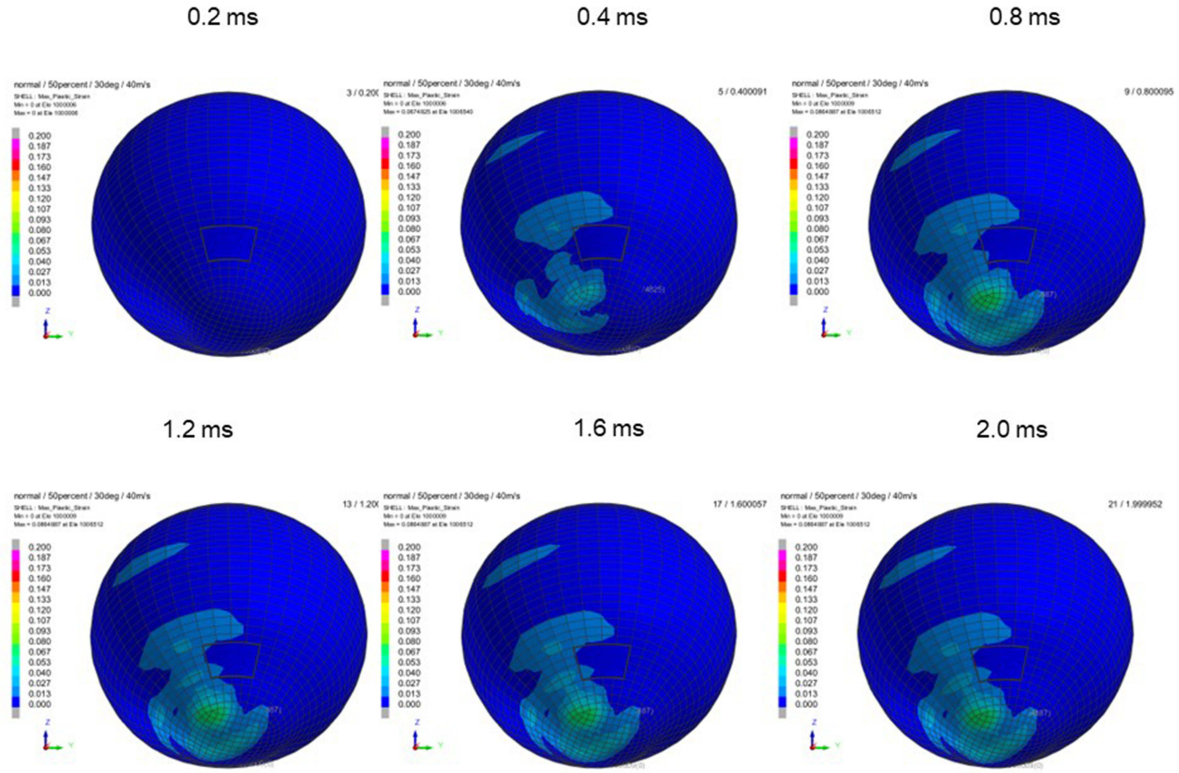

Figure 6 Sequential strain strength response of ocular surface of model eye upon airbag impact in 30°-gaze down position at 40 m/s with adhesion strength of scleral flap of 50%, shown at 0.4-ms intervals after 0.2 ms. Strain strength change is displayed in color as presented in the color bar scale (Figure 2).

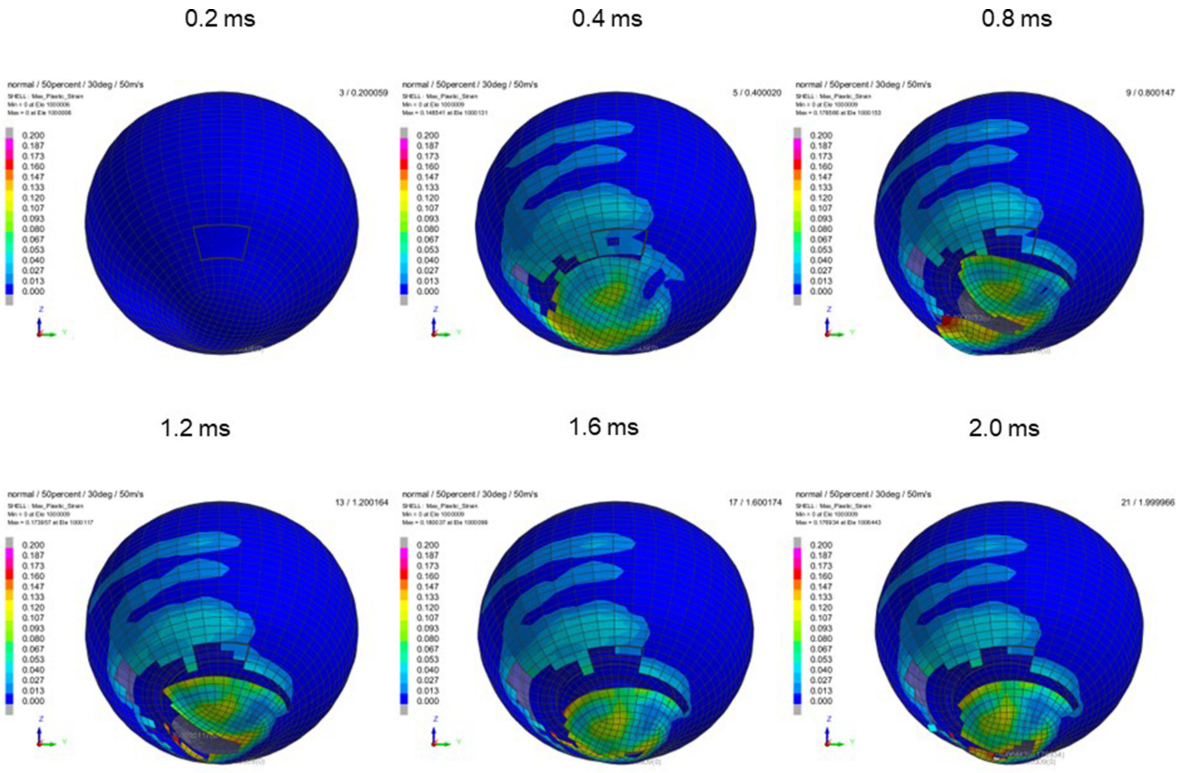

Figure 7 Sequential strain strength response of ocular surface of model eye upon airbag impact in 30°-gaze down position at 50 m/s with adhesion strength of scleral flap of 50%, shown at 0.4-ms intervals after 0.2 ms. Strain strength change is displayed in color as presented in the color bar scale (Figure 2).

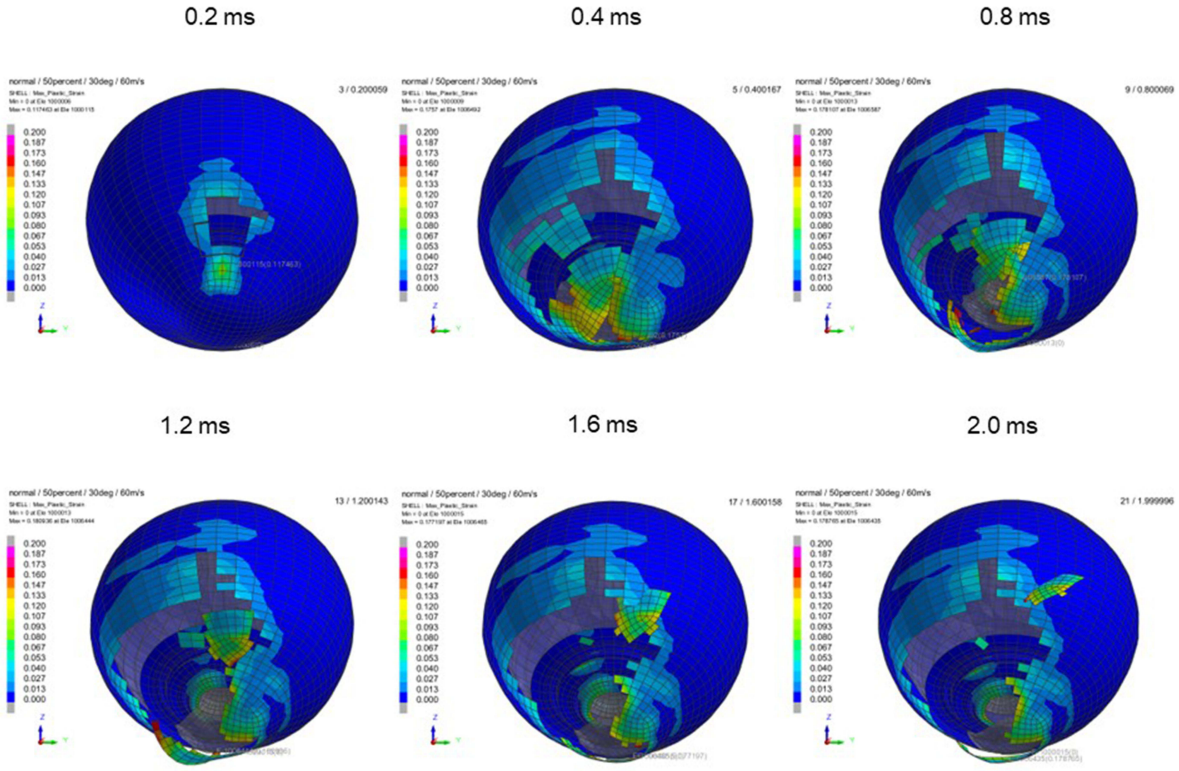

Figure 8 Sequential strain strength response of ocular surface of model eye upon airbag impact in 30°-gaze down position at 60 m/s with adhesion strength of scleral flap of 50%, shown at 0.4-ms intervals after 0.2 ms. Strain strength change is displayed in color as presented in the color bar scale (Figure 2).

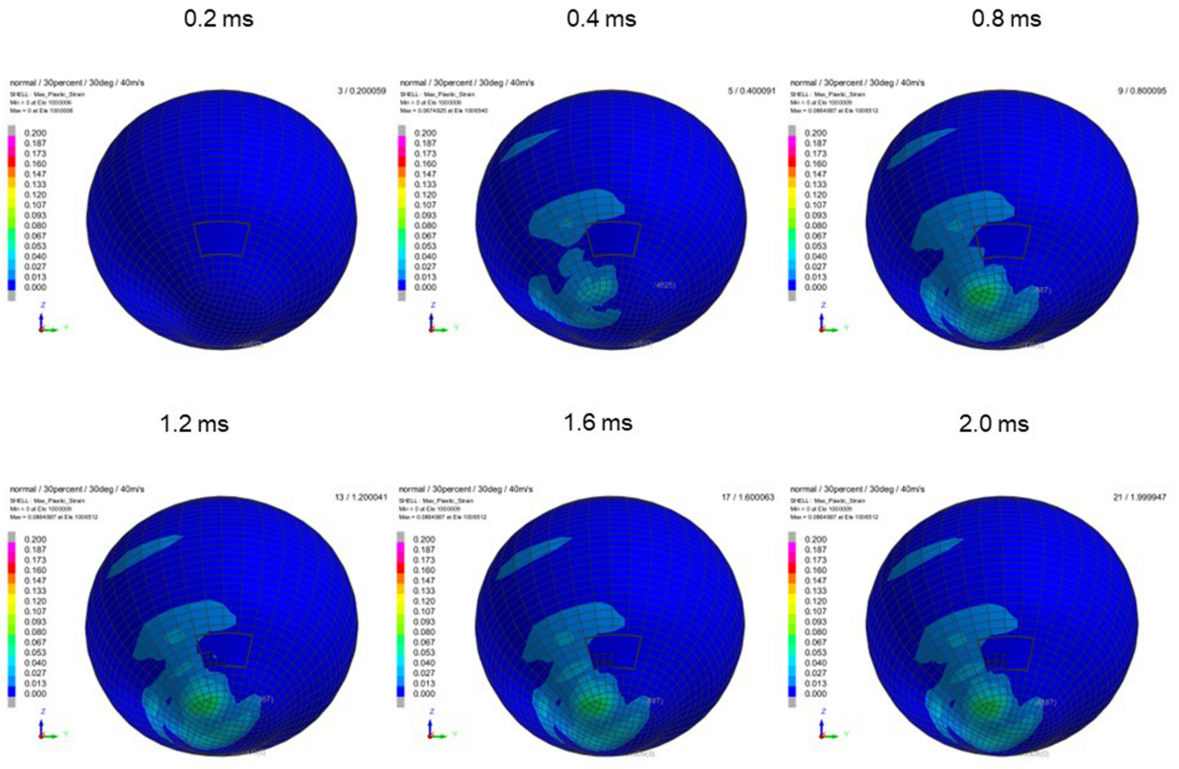

Figure 9 Sequential strain strength response of ocular surface of model eye upon airbag impact in 30°-gaze down position at 40 m/s with adhesion strength of scleral flap of 30%, shown at 0.4-ms intervals after 0.2 ms. Strain strength change is displayed in color as presented in the color bar scale (Figure 2).

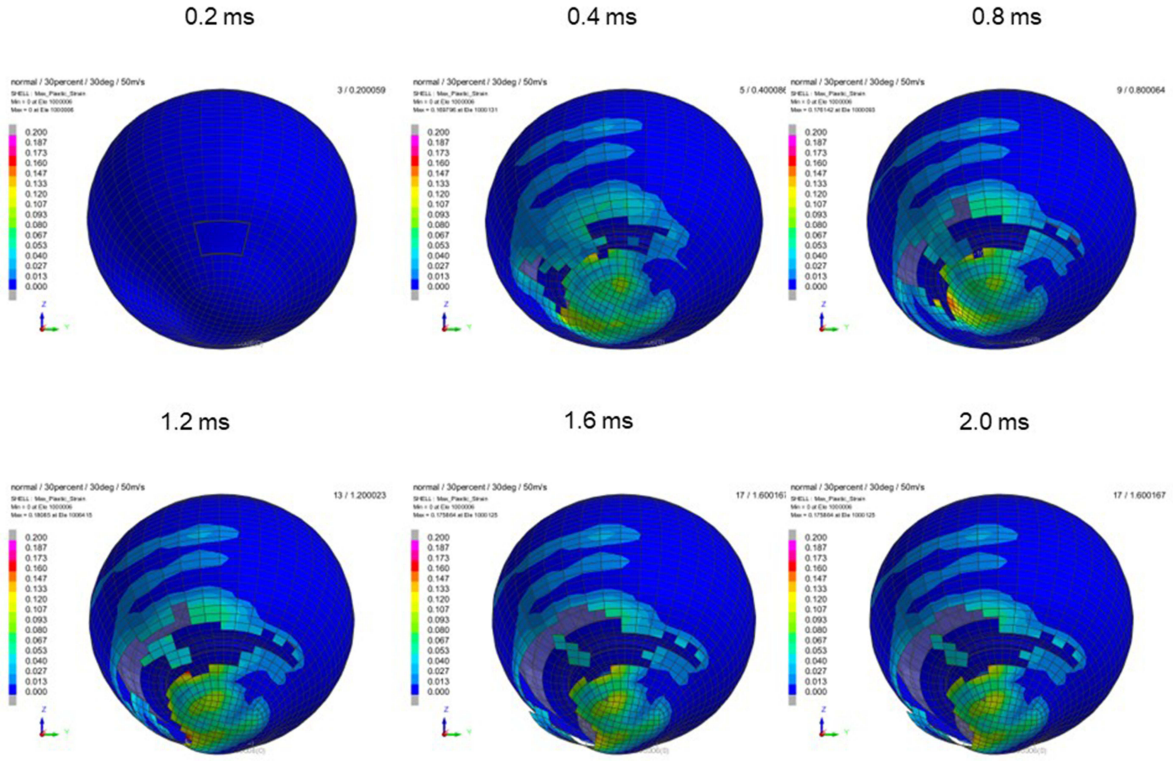

Figure 10 Sequential strain strength response of ocular surface of model eye upon airbag impact in 30°-gaze down position at 50 m/s with adhesion strength of scleral flap of 30%, shown at 0.4-ms intervals after 0.2 ms. Strain strength change is displayed in color as presented in the color bar scale (Figure 2).

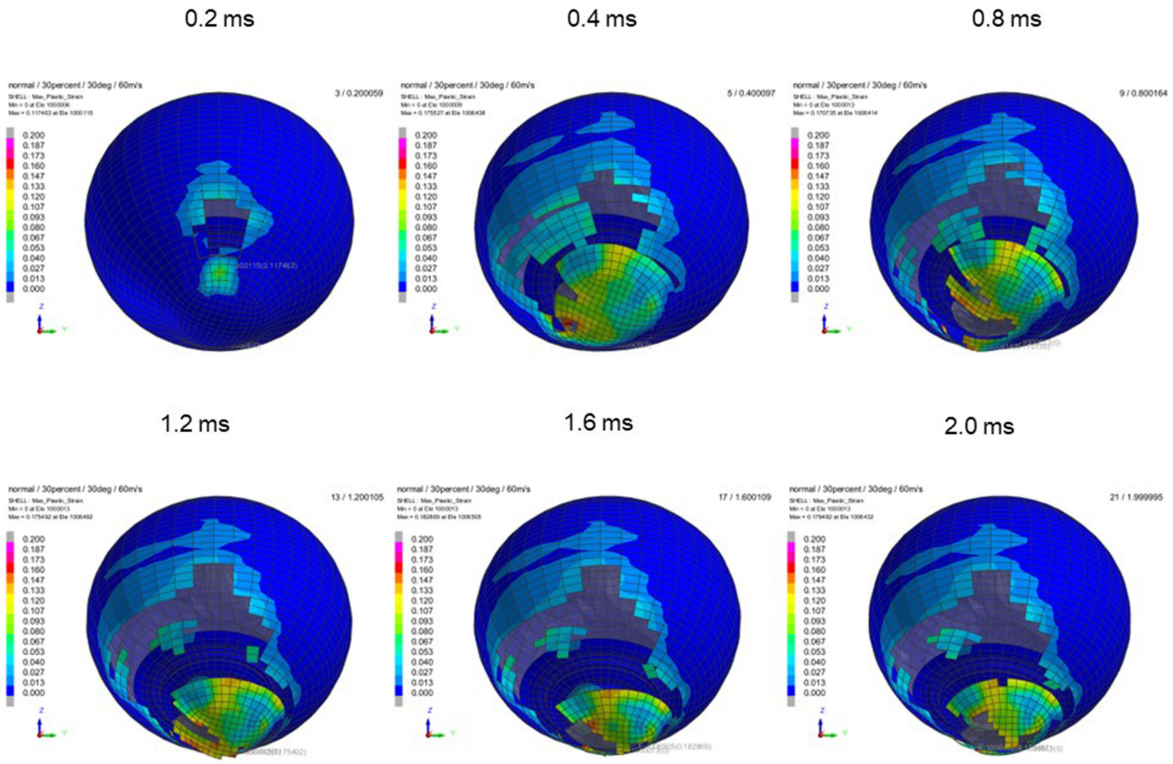

Figure 11 Sequential strain strength response of ocular surface of model eye upon airbag impact in 30°-gaze down position at 60 m/s with adhesion strength of scleral flap of 30%, shown at 0.4-ms intervals after 0.2 ms. Strain strength change is displayed in color as presented in the color bar scale (Figure 2).

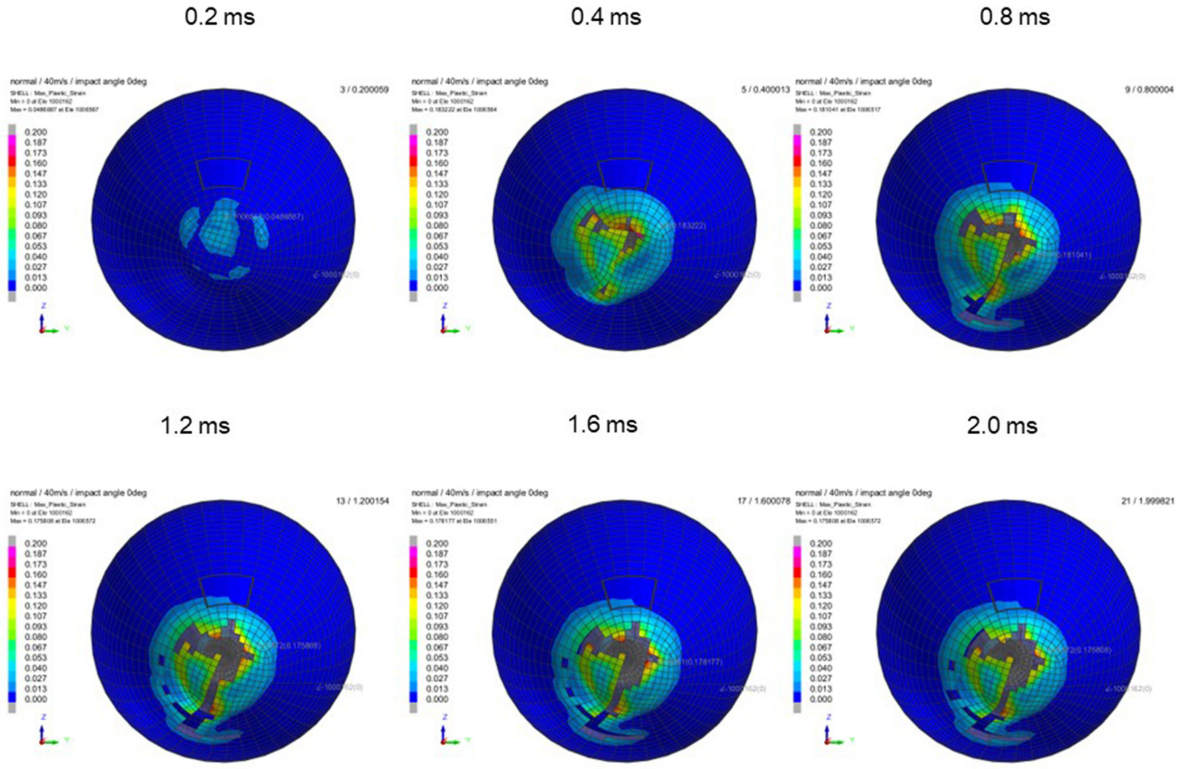

Figure 12 Sequential strain strength response of ocular surface of model eye upon airbag impact in straight position at 40 m/s with adhesion strength of scleral flap of 100%, shown at 0.4-ms intervals after 0.2 ms. Strain strength change is displayed in color as presented in the color bar scale (Figure 2).

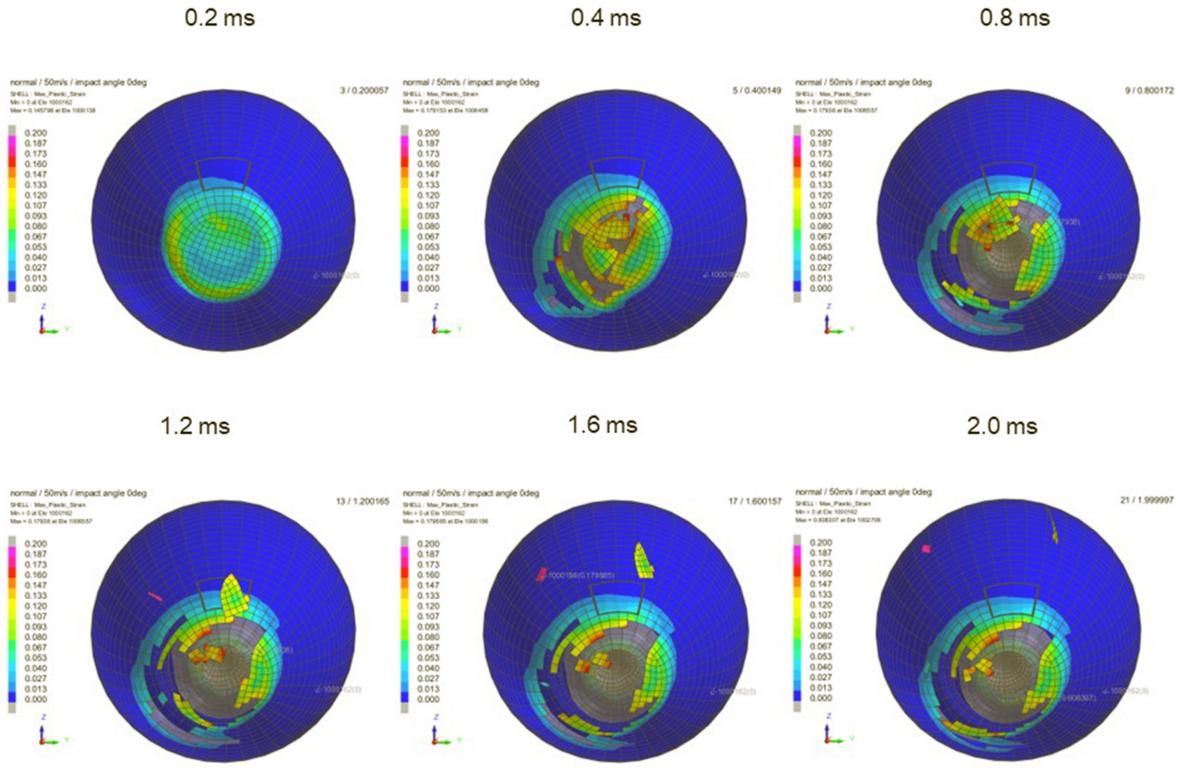

Figure 13 Sequential strain strength response of ocular surface of model eye upon airbag impact in straight position at 50 m/s with adhesion strength of scleral flap of 100%, shown at 0.4-ms intervals after 0.2 ms. Strain strength change is displayed in color as presented in the color bar scale (Figure 2).

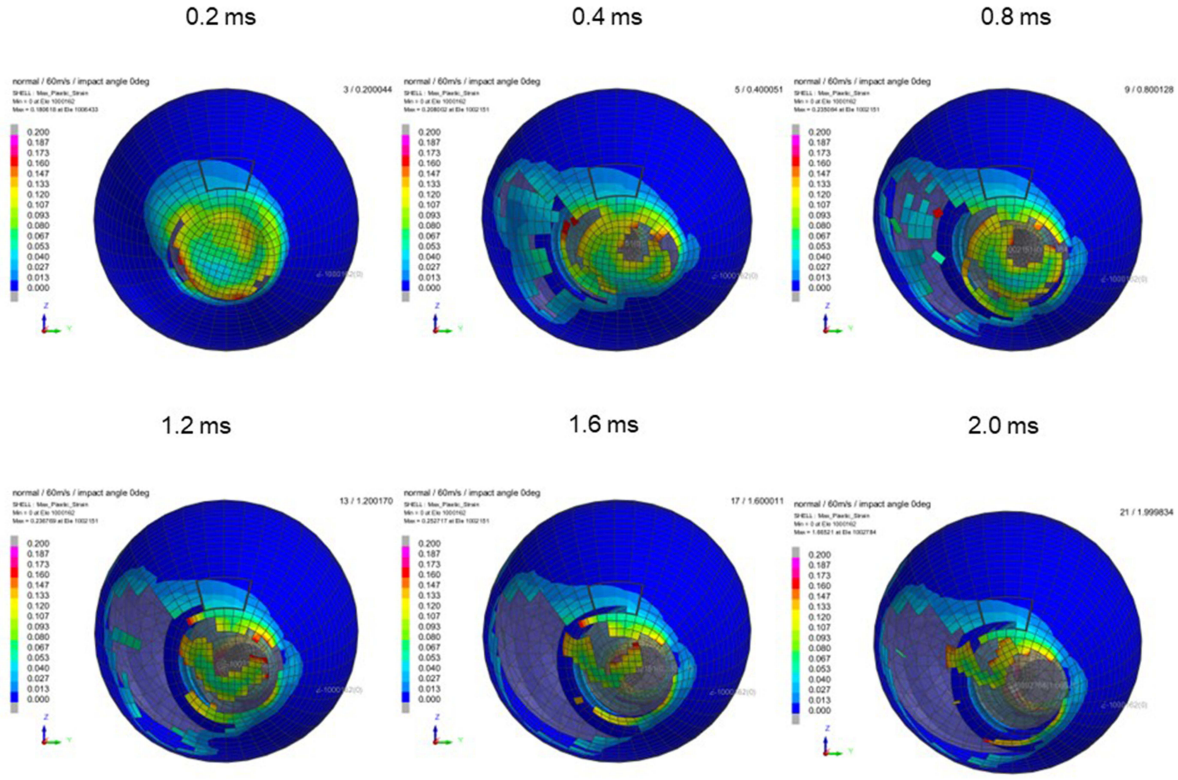

Figure 14 Sequential strain strength response of ocular surface of model eye upon airbag impact in straight position at 60 m/s with adhesion strength of scleral flap of 100%, shown at 0.4-ms intervals after 0.2 ms. Strain strength change is displayed in color as presented in the color bar scale (Figure 2).

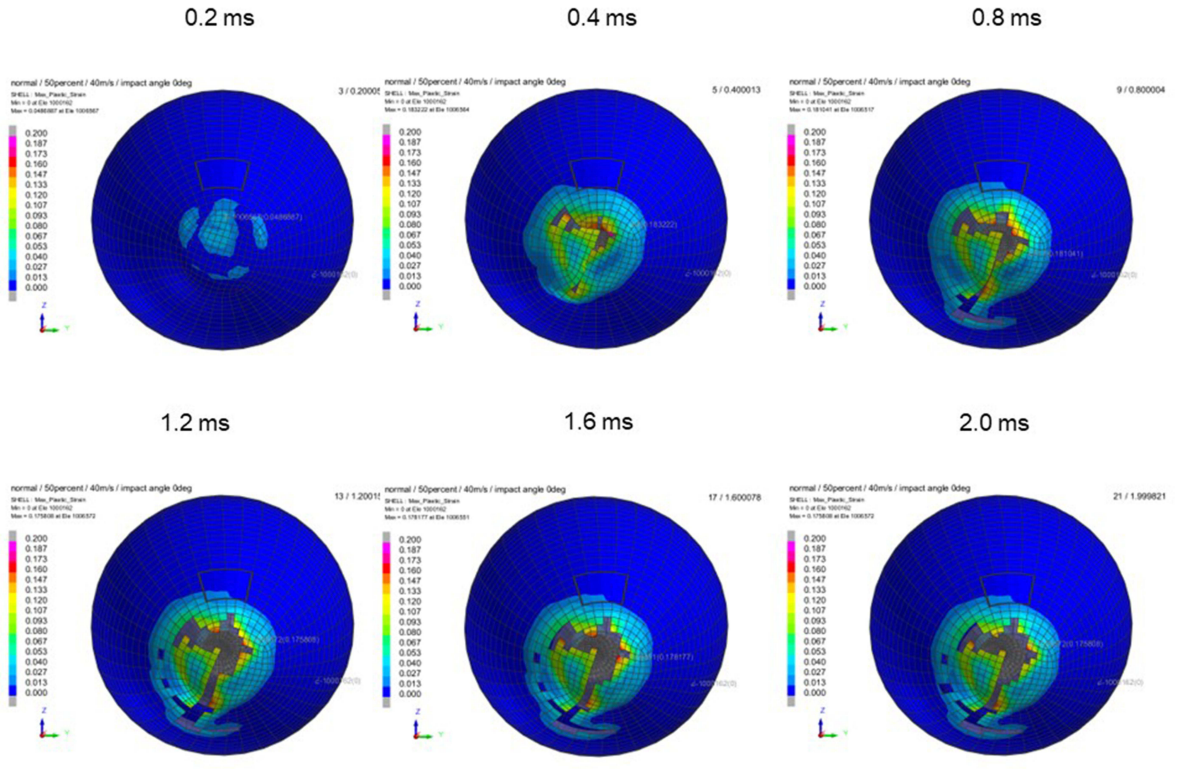

Figure 15 Sequential strain strength response of ocular surface of model eye upon airbag impact in straight position at 40 m/s with adhesion strength of scleral flap of 50%, shown at 0.4-ms intervals after 0.2 ms. Strain strength change is displayed in color as presented in the color bar scale (Figure 2).

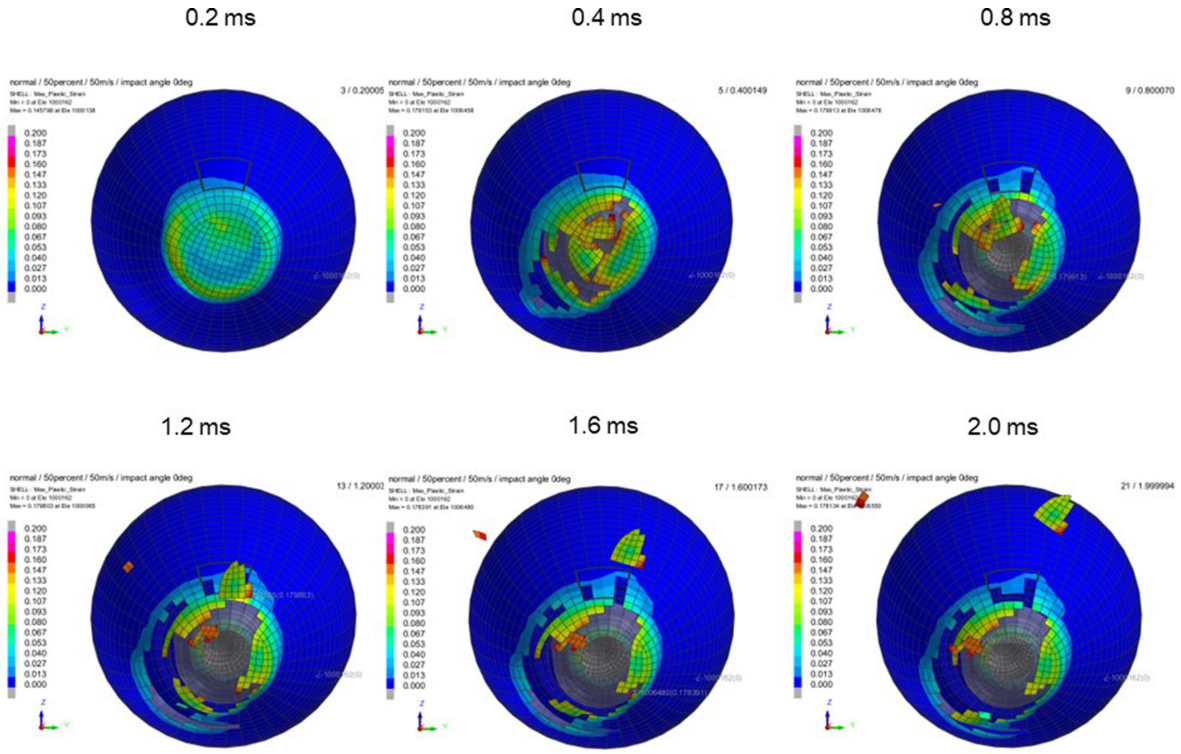

Figure 16 Sequential strain strength response of ocular surface of model eye upon airbag impact in straight position at 50 m/s with adhesion strength of scleral flap of 50%, shown at 0.4-ms intervals after 0.2 ms. Strain strength change is displayed in color as presented in the color bar scale (Figure 2).

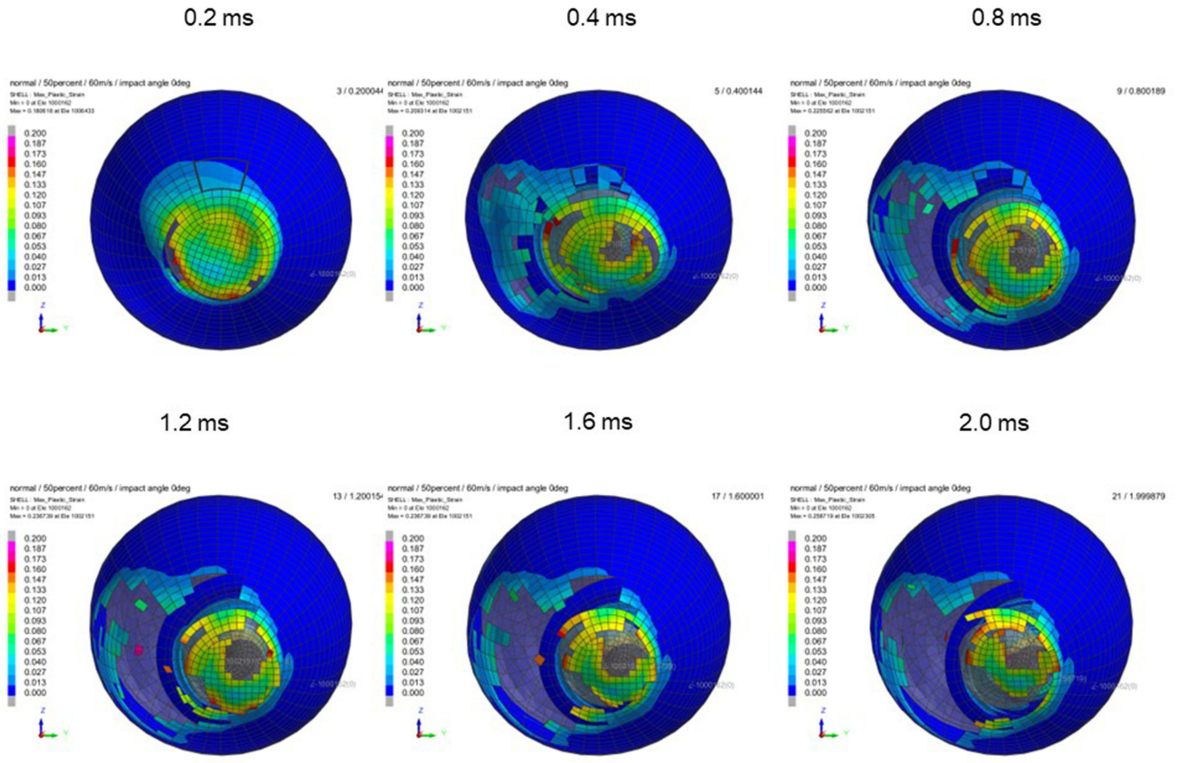

Figure 17 Sequential strain strength response of ocular surface of model eye upon airbag impact in straight position at 60 m/s with adhesion strength of scleral flap of 50%, shown at 0.4-ms intervals after 0.2 ms. Strain strength change is displayed in color as presented in the color bar scale (Figure 2).

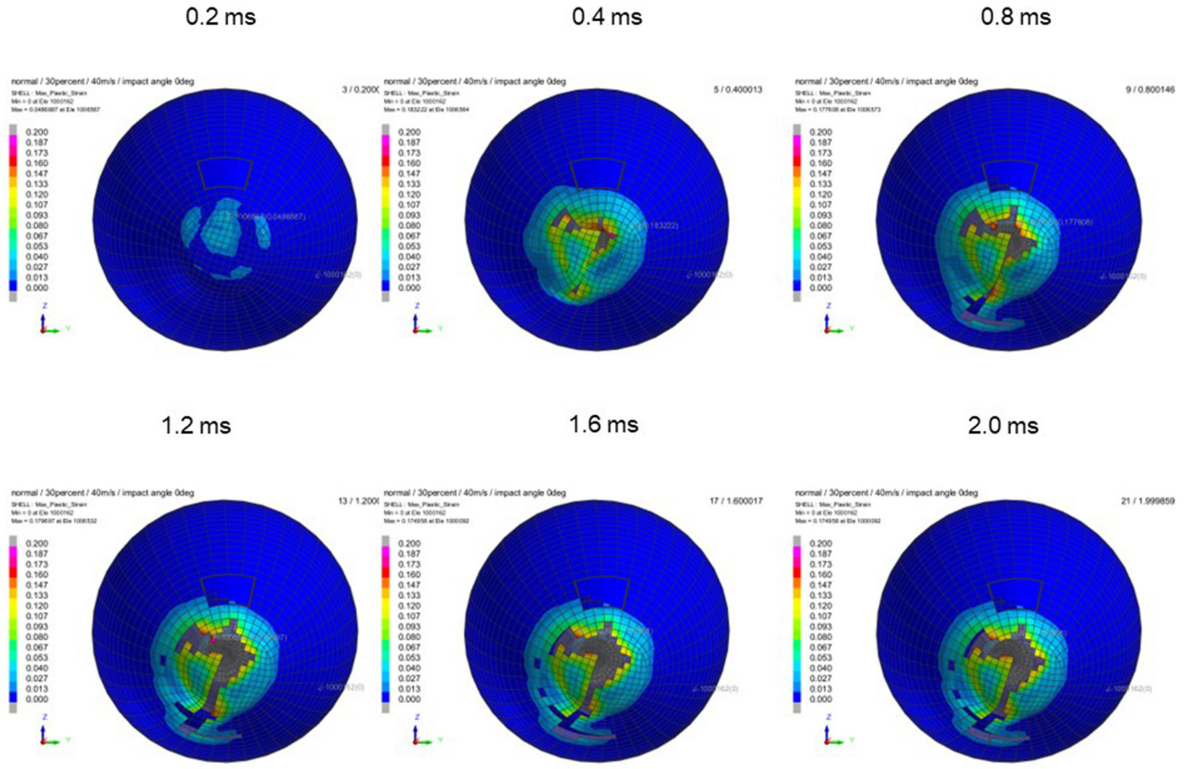

Figure 18 Sequential strain strength response of ocular surface of model eye upon airbag impact in straight position at 40 m/s with adhesion strength of scleral flap of 30%, shown at 0.4-ms intervals after 0.2 ms. Strain strength change is displayed in color as presented in the color bar scale (Figure 2).

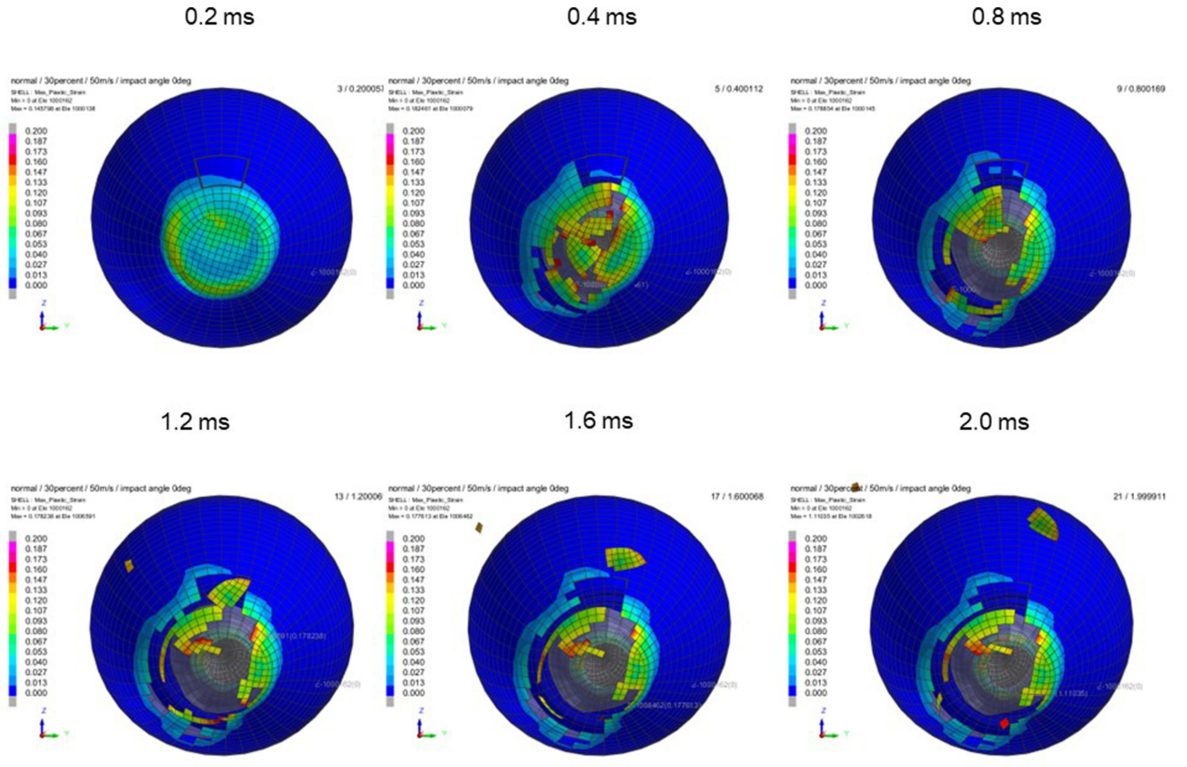

Figure 19 Sequential strain strength response of ocular surface of model eye upon airbag impact in straight position at 50 m/s with adhesion strength of scleral flap of 30%, shown at 0.4-ms intervals after 0.2 ms. Strain strength change is displayed in color as presented in the color bar scale (Figure 2).

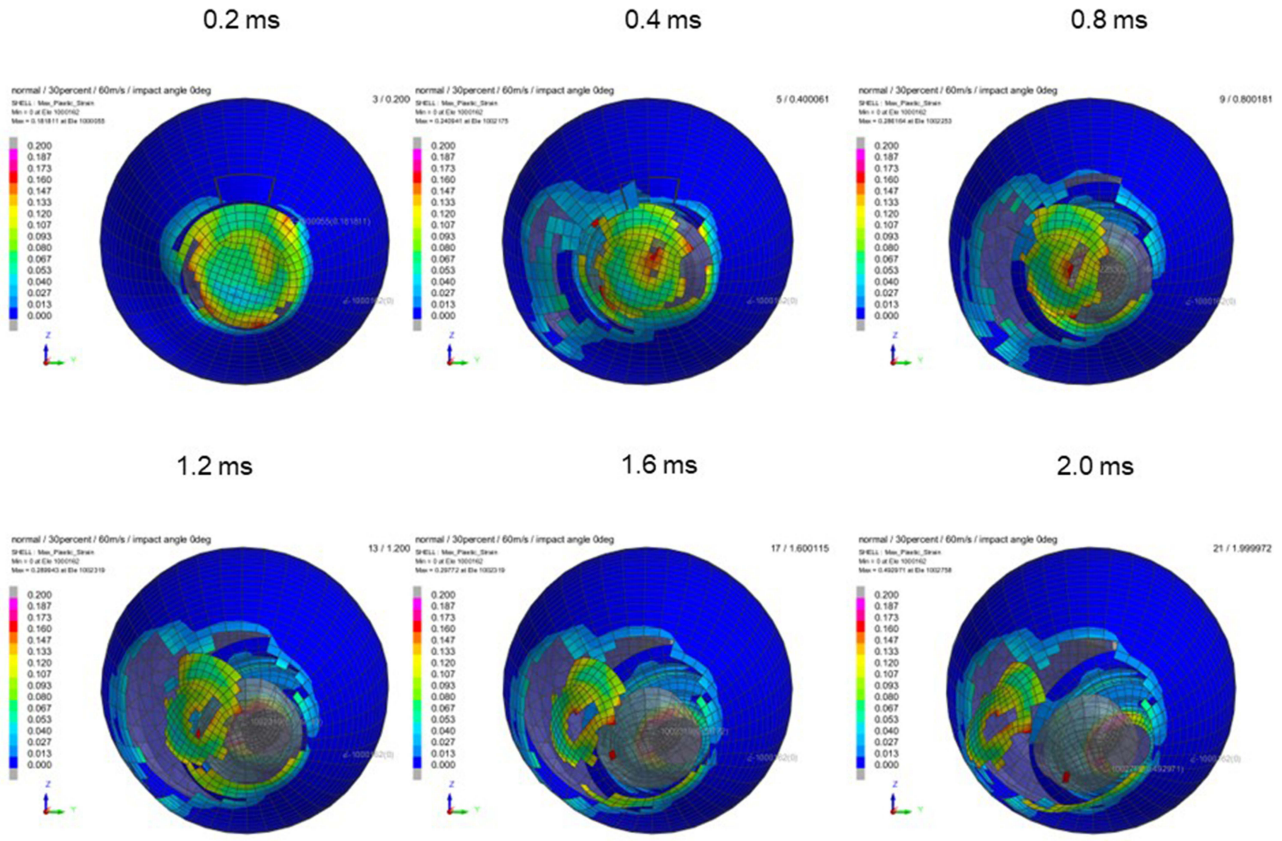

Figure 20 Sequential strain strength response of ocular surface of model eye upon airbag impact in straight position at 60 m/s with adhesion strength of scleral flap of 30%, shown at 0.4-ms intervals after 0.2 ms. Strain strength change is displayed in color as presented in the color bar scale (Figure 2).

impact velocities of 40 m/s or more in the 30° gaze-down position or straight position, and rupture of the scleral flap also resulted from extension of the corneal laceration through limbal damage (Figures 12, 14, 15, 17 and 18). Second, scleral rupture extending posteriorly from the scleral flap edge was observed at a high impact velocity (60 m/s) in the 30° gaze-down or straight positions in this simulation (Figures 3, 6, and 9).

The possibility of globe rupture due to injury to the sclera or cornea is shown for each scleral flap adhesion strength in Tables 1–3. In the case of 100% scleral flap adhesion strength, scleral flap rupture occurred at 50 m/s impact velocity in the 30° gaze-down position, while corneal rupture was observed at 40 m/s impact velocity in the straight position, and the earliest occurrence of globe rupture was 0.4 ms after the impact in this simulation (Table 1). Scleral flap rupture was observed at 40 m/s in both positions, and corneal rupture occurred at similar impact velocity in the case of 50% scleral flap adhesion strength (Table 2), but the earliest occurrence of globe rupture was 0.2 ms after the impact. In eyes with 30% scleral flap adhesion strength, scleral rupture was observed at an impact velocity of ≥40 m/s in both eyes, and corneal rupture occurred under conditions similar to those in eyes with 30% scleral flap strength (Table 3).

Discussion

In this study, we reported that considerable damage, such as corneal or scleral laceration, was observed, especially at higher airbag-impact velocities such as 40 m/s, 50 m/s, or 60 m/s, at any scleral flap adhesion strength. This seems reasonable because greater kinetic energy is derived from a higher airbag impact velocity. It is impossible to measure the impact velocity of an airbag on an eye. It is also not possible to determine the relationship between airbag impact velocity and ocular injury, or its relationship with clinical severity. The impact velocities of airbags on the eye range from 30 m/s to 66 m/s.[38] Airbag deployment occurs 15 ms after an impact, with complete expansion at 20–50 ms and deflation by 100 ms.[39,40] Automobile airbags are reported to deploy at a speed ranging from 81 kph to 322 kph (22–89 m/s).[37,39–41] From our present simulation study, globe rupture and scleral flap

Table 1 Possibility of Globe Rupture at Each Airbag-Impact Velocity and Occurrence of Laceration After Impact in Eyes with 100% Scleral Flap Adhesion Strength

Eye Position Impact Velocity (m/s)	Straight Position	30° Gaze Down Position
	Scleral flap	
20	Unlikely	Unlikely
30	Unlikely	Unlikely
40	Unlikely	Unlikely
50	Unlikely	0.8 ms
60	1.6 ms	0.4 ms
	Cornea	
20	Unlikely	Unlikely
30	Unlikely	Unlikely
40	0.4 ms	Unlikely
50	0.4 ms	1.0 ms
60	0.4 ms	0.8 ms

Table 2 Possibility of Globe Rupture at Each Airbag-Impact Velocity and Occurrence of Laceration After Impact in Eyes with 50% Scleral Flap Adhesion Strength

Eye Position Impact Velocity (m/s)	Straight Position	30° Gaze Down Position
	Scleral flap	
20	Unlikely	Unlikely
30	Unlikely	Unlikely
40	Unlikely	Unlikely
50	1.0 ms	0.8 ms
60	0.6 ms	0.2 ms
	Cornea	
20	Unlikely	Unlikely
30	Unlikely	Unlikely
40	0.4 ms	Unlikely
50	0.4 ms	0.8 ms
60	0.4 ms	0.4 ms

laceration occurred in all cases at an impact velocity of 60 m/s. Therefore, no additional velocities were examined in the simulations. Because the eyeball is viscoelastic, its response to an impact injury is rate-sensitive.[22] Therefore, we simulated impacts at various velocities within the range of deployment speed in this study to observe the biomechanical response for different scleral flap adhesion conditions. The critical threshold for globe rupture was presumed to be between 30 m/s and 40 m/s; however, scleral flap rupture could occur at an airbag impact velocity of 30 m/s if scleral flap adhesion was 30% (Table 3), indicating that special precautions should be considered in patients after trabeculectomy.

Blunt trauma occurring in a normal unoperated eye markedly differs from that in an eye where ocular rigidity is reduced by surgery.[31] It is difficult to measure scleral flap strength quantitatively in patients after trabeculectomy, and it is difficult to evaluate the rigidity of a scleral flap after trabeculectomy. Histopathologic analysis of scleral flap tissues demonstrated disorganized, loose connective tissue with an absence of fibroblasts and disorganization of collagen with large spaces between fibrils; these findings

Table 3 Possibility of Globe Rupture at Each Airbag-Impact Velocity and Occurrence of Laceration After Impact in Eyes with 30% Scleral Flap Adhesion Strength

Eye Position Impact Velocity (m/s)	Straight Position	30° Gaze Down Position
	Scleral flap	
20	Unlikely	Unlikely
30	Unlikely	Unlikely
40	0.6 ms	1.0 ms
50	0.6 ms	0.4 ms
60	0.4 ms	0.2 ms
	Cornea	
20	Unlikely	Unlikely
30	Unlikely	Unlikely
40	0.4 ms	Unlikely
50	0.4 ms	0.6 ms
60	0.4 ms	0.4 ms

suggest that normal tissue architecture is completely destroyed in the scleral flap.[18] The reduction in scleral fibroblast cellularity may be related to abnormalities of mucopolysaccharides and disorganization of the characteristic lamellar organization of collagen fibrils in the sclera, thereby increasing the friability of the scleral flap.[18] Using polarization-sensitive optical coherence tomography revealed local birefringence, indicating areas without fibrosis, around the scleral flap in patients who underwent trabeculectomy.[42] Comparing the possibility of globe rupture among scleral flap adhesion strengths in our model, a difference was evident in the scleral flap; in contrast, no apparent difference was found in the cornea (Tables 1–3) in any eye position. Combined with the above findings, it is notable that scleral flap is the most important risk factor for blunt trauma to the eye after trabeculectomy. If the critical threshold could be determined by a more detailed modelling of scleral flap adhesion (60%, 70%, 80%, etc.) in a future study, this could be an important result. Several cases of blunt trauma to the eye following trabeculectomy have been reported;[15,20,21] however, the process of ocular injury in these eyes during the minute period following an object impact has not been reported.

We observed two interesting phenomena during the process of injury development in this simulation study. First, as shown in the results, scleral rupture extended across the edge of the scleral flap posteriorly at a high airbag impact velocity (60 m/s) in the 30° gaze-down position (Figures 5, 8, 11). Several cases developed a scleral laceration, including scleral flap dehiscence extending posteriorly after trabeculectomy, and all of them required surgical repair.[19,21] This posterior extension of the scleral flap has a similar pattern of injury to that in eyes that have undergone trabeculectomy, as identified in our simulated results.

Second, rupture of the scleral flap followed by extension of a corneal laceration through limbal damage (Figures 12, 14, 15, 17 and 18) resulted from a different mechanism than that of direct injury to the incised region. It is reported that blunt trauma causes stretching of limbal tissues, equatorial scleral expansion and acute elevation of IOP, with consequent tearing of the tissue near the anterior chamber angle,[31] and this resulted in traumatic aniridia in a pseudophakic patient after trabeculectomy.[31] These sequences of events are likely to occur in patients with low ocular rigidity after trabeculectomy,[31] and this can be applied to the so-called secondary scleral flap rupture in our simulated study. These results indicate that FEA investigation of airbag-induced injury of the eye after trabeculectomy provides important clues to more precisely explain the mechanism of tissue damage over an ultrashort period, together with the findings in reported clinical cases.

Despite our careful calculations using the simulation model, there are still limitations to our study. First, the scleral flap was sutured clinically; however, we simulated the adhesion of the scleral flap and surrounding sclera at three strengths, 30%, 50%, and 100%, in this study. Thirty percent strength mimicked cases that had undergone laser suture lysis, and 100% strength indicated complete wound healing after a considerable number of days. Fifty percent strength was used to simulate the

intermediate state between 30% and 100%, and considering these relatively rough states, more detailed study of adhesion strength, in a linear stepwise manner, would provide more useful information as mentioned previously.

Second, regarding the design of the scleral flap, two points differed from the clinical situation. A hinge segment located at the posterior end of the flap was not included in this study, and the shape of the scleral flap was a trapezoid with lower base of 3.6 mm, upper base of 5.0 mm, and both lateral sides of 3.0 mm in this simulation due to the scleral mesh size. A hinge segment can be simulated by setting the scleral flap adhesion strength of that line to 100%, even in 30% or 50% adhesion strength situations, which will be applied in future studies.

Third, mechanical and anatomical involvement of the conjunctiva was not considered in this simulation. Several cases of conjunctival bleb injury due to blunt trauma have been reported previously.[43–45] It is true that scleral flap injury usually occurs following conjunctival damage, and the mechanical factors of a conjunctival bleb may influence scleral flap trauma. However, the conjunctiva is very thin and its physiological properties have not yet been clarified. Therefore, for simplicity, we did not include the conjunctiva as an element of the eyeball in the simulation. Exclusion of the eyelid in this model to reduce calculation time might also have some influence on the results obtained in this study. Cirovic et al carried out simulation research on optic nerve blunt trauma using an FEA model including the optic nerve, muscles and orbital fat;[46] however, we found no FEA study including the eyelid as an element. The present eye model is composed based on reliable anatomical and geometrical information from past studies; however, we also have made simplifications to the model which lacks several variables, because modeling with FEA as part of a larger overall model of the eye would require extremely fine mesh, leading to a very computationally expensive model. The internal contacts between tissues in the eye have not been characterized and are therefore not well defined in our FEA model, but these variables in the minute condition of the modeled eyeball should be taken into consideration in a future study. Watson et al reported that areas of maximum stress were found in the thinnest section of the sclera, adjacent to the vitreous base in blast injury simulations using an FEA porcine eye model.[47]

In conclusion, we believe that our goal of assessing the mechanical properties of eyes impacted by an airbag that have undergone trabeculectomy was achieved by demonstrating that corneoscleral laceration, including serious scleral flap damage, might occur at higher impact velocities (40 m/s or more) with greater susceptibility in the 30° gaze-down position. Considering that there are few reports of cases of serious blunt trauma by an airbag impact after trabeculectomy, our results may have important meanings for patients who have undergone cataract surgery with an incision at the corneoscleral border. The present results emphasize the necessity of wearing a seatbelt and eye protection, such as glasses, to prevent serious ocular injury, especially in high-risk populations, such as short-stature individuals with glaucoma who have undergone trabeculectomy, even when sitting in passenger seats.

Acknowledgments

This work was supported by a Grant-in-Aid for Encouragement of Scientists (21K09709) from the Ministry of Education, Science, Sports, and Culture of Japan. We thank Dr W Gray for editing this manuscript.

Funding

The authors have no relevant financial or non-financial interests to disclose for this work.

Disclosure

The authors have no competing interests to declare that are relevant to the content of this article.

References

1. Zador PL, Ciccone MA. Automobile driver fatalities in frontal impacts:Airbags compared with manual belts. *Am J Public Health*. 1993;83(5):661–666. doi:10.2105/AJPH.83.5.661
2. Segui-Gomez M, Levy J, Roman H, Thompson KM, McCabe K, Graham JD. Driver distance from the steering wheel: perception and objective measurement. *Am J Public Health*. 1999;89(7):1109–1111. doi:10.2105/AJPH.89.7.1109
3. Manche EE, Goldberg RA, Mondino BJ. Airbag-related ocular injuries. *Ophthalmic Surg Lasers*. 1997;28(3):246–250. doi:10.3928/1542-8877-19970301-15
4. Duma SM, Kress TA, Porta DJ, et al. Airbag-induced eye injuries:A report of 25 cases. *J Trauma*. 1996;41(1):114–119. doi:10.1097/00005373-199607000-00018

5. de Vries S, Geerards AJ. Long-term sequelae of isolated chemical "airbag" keratitis. *Cornea*. 2007;26(8):998–999. doi:10.1097/ICO.0b013e3180ca9a35
6. Baker RS, Flowers CW, Singh P, Smith A, Casey R. Corneoscleral laceration caused by airbag trauma. *Am J Ophthalmol*. 1996;121(6):709–711. doi:10.1016/S0002-9394(14)70639-7
7. Lesher MP, Durrie DS, Stiles MC. Corneal edema, hyphema, and angle recession after air bag inflation. *Arch Ophthalmol*. 1993;111(10):1320–1322. doi:10.1001/archopht.1993.01090100026014
8. Onwuzuruigbo CJ, Fulda GJ, Larned D, Hailstone D. Traumatic blindness after airbag deployment: bilateral lenticular dislocation. *J Trauma*. 1996;40(2):314–316. doi:10.1097/00005373-199602000-00029
9. Zabriskie NA, Hwang IP, Ramsey JF, Crandall AS. Anterior lens capsule rupture caused by air bag trauma. *Am J Ophthalmol*. 1997;123(6):832–833. doi:10.1016/S0002-9394(14)71133-X
10. Wang SH, Lim CC, Teng YT. Airbag-associated severe blunt eye injury causes choroidal rupture and retinal hemorrhage: a case report. *Case Rep Ophthalmol*. 2017;8(1):13–20. doi:10.1159/000452652
11. Ruiz-Moreno JM. Air bag-associated retinal tear. *Eur J Ophthalmol*. 1998;8(1):52–53. doi:10.1177/112067219800800112
12. Eliott D, Hauch A, Kim RW, Fawzi A. Retinal dialysis and detachment in a child after airbag deployment. *J AAPOS*. 2011;15(2):203–204. doi:10.1016/j.jaapos.2010.11.021
13. Salam T, Stavrakas P, Wickham L, Bainbridge J. Airbag injury and bilateral globe rupture. *Am J Emerg Med*. 2010;28(8):982.e5–982.e6. doi:10.1016/j.ajem.2009.12.015
14. Bar-David L, Blumenthal EZ. Evolution of glaucoma surgery in the last 25 years. *Rambam Maimonides Med J*. 2018;9(3):e0024. doi:10.5041/RMMJ.10345
15. Gungor SG, Sezenoz AS, Eksioglu U, Akman A. Scleral flap wound dehiscence with Valsalva maneuver after trabeculectomy with mitomycin C. *Beyoglu Eye J*. 2022;7(3):231–236. doi:10.14744/bej.2022.34711
16. Bindlish R, Condon GP, Schlosser JD, D'Antonio J, Lauer KB, Lehrer R. Efficacy and safety of mitomycin-C in primary trabeculectomy: five-year follow-up. *Ophthalmology*. 2002;109(7):1336–1341. doi:10.1016/S0161-6420(02)01069-2
17. Prata JA, Seah SK, Minckler DS, Baerveldt G. Postoperative complications and short-term outcome after 5-fluorouracil or mitomycin-C trabeculectomy. *J Glaucoma*. 1995;4(1):25–31. doi:10.1097/00061198-199502000-00007
18. Nuyts RM, Felten PC, Pels E, et al. Histopathologic effects of mitomycin C after trabeculectomy in human glaucomatous eyes with persistent hypotony. *Am J Ophthalmol*. 1994;118(2):225–237. doi:10.1016/S0002-9394(14)72903-4
19. Zeiter JH, Shin DH. Traumatic rupture of the globe after glaucoma surgery. *Am J Ophthalmol*. 1990;109(6):732–733. doi:10.1016/S0002-9394(14)72447-X
20. Rubinstein A, Salmon JF. Late traumatic scleral flap dehiscence following trabeculectomy. *Eye (Lond)*. 2007;21(1):145–146. doi:10.1038/sj.eye.6702476
21. Shah BP, Clarke J. Donor pericardium graft repair of traumatic globe rupture at previous trabeculectomy site. *Digit J Ophthalmol*. 2014;20(3):48–50. doi:10.5693/djo.02.2013.09.003
22. Viano DC, King AI, Melvin JW, Weber K. Injury biomechanics research: an essential element in the prevention of trauma. *J Biomech*. 1989;2(5):403–417. doi:10.1016/0021-9290(89)90201-7
23. Uchio E, Ohno S, Kudoh J, Aoki K, Kisielewicz LT. Simulation model of an eyeball based on finite element analysis on a supercomputer. *Br J Ophthalmol*. 1999;83(10):1106–1111. doi:10.1136/bjo.83.10.1106
24. Uchio E, Kadonosono K, Matsuoka Y, Goto S. Simulation of airbag impact on an eye with transsclerally fixated posterior chamber intraocular lens using finite element analysis. *J Cataract Refract Surg*. 2004;30(2):483–490. doi:10.1016/S0886-3350(03)00520-0
25. Uchio E, Ohno S, Kudoh K, Kadonosono K, Andoh K, Kisielewicz LT. Simulation of airbag impact on post-radial keratotomy eye using finite element analysis. *J Cataract Refract Surg*. 2001;27(11):1847–1853. doi:10.1016/S0886-3350(01)00966-X
26. Uchio E, Watanabe Y, Kadonosono K, Matsuoka Y, Goto S. Simulation of airbag impact on eyes after photorefractive keratectomy by finite element analysis method. *Graefes Arch Clin Exp Ophthalmol*. 2003;241(6):497–504. doi:10.1007/s00417-003-0679-8
27. Huang J, Uchio E, Goto S. Simulation of airbag impact on eyes with different axial lengths after transsclerally fixated posterior chamber intraocular lens by using finite element analysis. *Clin Ophthalmol*. 2015;9:263–270. doi:10.2147/OPTH.S75180
28. Okamura K, Shimokawa A, Takahashi R, Saeki Y, Ozaki H, Uchio E. Finite element analysis of air gun impact on post-keratoplasty eye. *Clin Ophthalmol*. 2020;14:179–186. doi:10.2147/OPTH.S236825
29. Takahashi R, Okamura K, Tsukahara-Kawamura T, et al. Finite element analysis of changes in tensile strain by airsoft gun impact on eye and deformation rate in eyes of various axial lengths. *Clin Ophthalmol*. 2020;14:1445–1450. doi:10.2147/OPTH.S249483
30. Kobayashi A, Izaki R, Fujita H, et al. Finite element analysis of changes in tensile strain and deformation by airbag impact in eyes of various axial lengths. *Int Ophthalmol*. 2022;43(7):2143–2151. doi:10.1007/s10792-022-02609-7
31. Kaliaperumal S, Troutbeck R, Iemsomboon W, Farinelli A. Isolated traumatic aniridia after trabeculectomy in a pseudophakic eye. *Indian J Ophthalmol*. 2014;62(3):371–372. doi:10.4103/0301-4738.109515
32. Bhavsar AR, Chen TC, Goldstein DA. Corneoscleral laceration associated with passenger side airbag inflation. *Br J Ophthalmol*. 1997;81(6):514–515. doi:10.1136/bjo.81.6.513b
33. Buzard KA. Introduction to biomechanics of the cornea. *Refract Corneal Surg*. 1992;8(2):127–138. doi:10.3928/1081-597X-19920301-07
34. Greene PR. Closed-form ametropic pressure-volume and ocular rigidity solutions. *Am J Optom Physiol Opt*. 1985;62(12):870–878. doi:10.1097/00006324-198512000-00008
35. Ruan JS, Pradad P. Coupling of a finite element human head model with a lumped parameter Hybrid III dummy model: preliminary results. *J Neurotrauma*. 1995;12(4):725–734. doi:10.1089/neu.1995.12.725
36. Kim JM, Kim KO, Kim YD, Choi GJ. A case of air-bag associated severe ocular injury. *Korean J Ophthalmol*. 2004;18(1):84–88. doi:10.3341/kjo.2004.18.1.84
37. Schreck RM, Rouhana SW, Santrock J, et al. Physical and chemical characterization of airbag effluents. *J Trauma*. 1995;38(4):528–532. doi:10.1097/00005373-199504000-00011
38. Duma SM, Kress TA, Porta DJ, Simmons RJ, Alexander CL, Woods CD. Airbag-induced eye injuries: experiments with in situ cadaver eyes. *Biomed Sci Instrum*. 1997;33:106–111.

39. National Highway Traffic Safety Administration. *Air Bag Deployment Characteristics*. Springfield, VA: National Technical Information Service; 1992.
40. Fukagawa K, Tsubota K, Kimura C, et al. Corneal endothelial cell loss induced by airbags. *Ophthalmology*. 1993;100(12):1819–1823. doi:10.1016/S0161-6420(13)31394-3
41. Ball DC, Bouchard CS. Ocular morbidity associated with airbag deployment: a report of seven cases and a review of the literature. *Cornea*. 2001;20(2):159–163. doi:10.1097/00003226-200103000-00009
42. Fukuda S, Fujita A, Kasaragod D, et al. Comparison of intensity, phase retardation, and local birefringence images for filtering blebs using polarization-sensitive optical coherence tomography. *Sci Rep*. 2018;8(1):7519. doi:10.1038/s41598-018-25884-w
43. Kahook MY, Noecker RJ, Abdelghani WM, Schuman JS. Filtering bleb rupture after intravitreal triamcinolone acetonide injection. *Ophthalmic Surg Lasers Imaging*. 2008;39(3):232–233. doi:10.3928/15428877-20080501-08
44. Greenfield DS. Bleb rupture following filtering surgery with mitomycin-C: clinicopathologic correlations. *Ophthalmic Surg Lasers*. 1996;27(10):876–877. doi:10.3928/1542-8877-19961001-12
45. Greenfield DS, Liebmann JM, Jee J, Ritch R. Late-onset bleb leaks after glaucoma filtering surgery. *Arch Ophthalmol*. 1998;116(4):443–447. doi:10.1001/archopht.116.4.443
46. Cirovic S, Bhola RM, Hose DR, et al. Computer modelling study of the mechanism of optic nerve injury in blunt trauma. *Br J Ophthalmol*. 2006;90(6):778–783. doi:10.1136/bjo.2005.086538
47. Watson R, Gray W, Sponsel WE, et al. Simulations of porcine eye exposure to primary blast insult. *Transl Vis Sci Technol*. 2015;25(4):8. doi:10.1167/tvst.4.4.8